Epigenetic alterations associated with dexamethasone sodium phosphate through DNMT and TET in RPE cells

Wenjie Liu,[1, 2] Sruthi Priya Mohan,[3] Nareshkumar Ragavachetty Nagaraj,[3] Shyam Sundar Jaganathan,[3] Yi Wen,[1, 2] Sharada Ramasubramanyan,[3] Joseph Irudayaraj[1, 2]

[1]*Department of Bioengineering, Cancer Center at Illinois, Micro and Nanotechnology Laboratory. University of Illinois at Urbana-Champaign, Urbana, IL;* [2]*Biomedical Research Center in Mills Breast Cancer Institute, Carles Foundation Hospital, Urbana, IL;* [3]*R.S. Mehta Jain Department of Biochemistry and Cell Biology, KBIRVO, Vision Research Foundation, Chennai, TN, India*

Purpose: To elucidate the mechanism behind epigenetic alteration associated with dexamethasone (DEX) sodium phosphate treatment.
Methods: We performed enzyme-linked immunosorbent assay to quantify changes in global DNA methylation and hydroxymethylation, quantitative real-time PCR (qRT-PCR) of the DNA methylation- and hydroxymethylation-related gene, in vitro DNA methyltransferase (DNMT) enzymatic activity assays with purified DNMTs, and DNA hydroxymethylation pattern with super-resolution imaging.
Results: We identified global DNA hypomethylation and hyper-hydroxymethylation upon DEX treatment, associated with aberrant mRNA expression levels of DNMT and ten-eleven translocation (TET) proteins. Additionally, DEX exposure could directly hinder DNMT activities.
Conclusions: We showed that DEX-induced epigenetic alterations are linked to aberrant DNMT and TET expression, potentially through an essential role of DNMT.

Glucocorticoids remain the most conventional mode of treatment in treating ocular retinopathies, such as macular edema due to pseudophakia [1,2], choroidal neovascularization [3,4], uveitis [5], diabetes retinopathy [6,7], and retinal vein occlusion [8,9], because of their anti-inflammatory, immunosuppressive, and antiangiogenic effects. Although intravitreal steroids, such as fluocinoloneacetonide, triamcinolone acetonide, and dexamethasone (DEX), are in use for treatment of the conditions above, these steroids were found to be significantly different in their mechanism of action in aqueous and lipid solubility, delivery system requirements, pharmacokinetics, and interactions with glucocorticoid receptors [10]. Intravitreal administration of dexamethasone (DEX), in the form of an intravitreal implant containing 0.7 mg drug in a solid polymer drug delivery system (OZURDEX, Allergan, CA) for sustained release, is proposed as a standard treatment. Many clinical studies demonstrate that the drug is well-tolerated and produces improvements in visual acuity, macular thickness, fluorescein leakage [11-14], and effective immunosuppression after epiretinal transplantation [15]. However, it must be noted that long-term exposure could cause elevation of intraocular pressure (IOP), cataract formation, endophthalmitis uveitis, or the altered immune system [1,16-22]. Not limited to ocular pathology, adverse effects of glucocorticoids in the development of many neurologic and immunological diseases warrant caution regarding long-term use of these drugs [23]. Several possible mechanisms for adverse steroid response have been studied, and the proposed mechanisms include deposition of extracellular matrix material [24], decreased protease and stromelysin activities [25,26], reorganization of the trabecular meshwork (TM) cytoskeleton [27,28], increased nuclear size and DNA content [29], decreased phagocytotic capacity [30], and change in the synthesis of specific proteins [31].

However, few in vitro studies have explored the role of DEX in protecting human RPE cells from oxidative stress [32] and retinal ganglion cells from cell death [33]. Although examination of the effect of DEX in ocular therapeutics is relatively well-established, only recently have studies explored DEX in epigenetics-mediated mechanisms [34,35]. The mode of action of how DEX mediates the epigenome to impart therapy in diseases of the eye is a gap in the field.

Gene expression in mammalian cells depends on multiple epigenetic modifications of regulated chromatin states. Types of epigenetic modifications include DNA methylation [36], RNA methylation [37], histone modifications [38], and small non-coding RNAs [39], among others. DNA methylation is

Correspondence to: Joseph Irudayaraj, Department of Bioengineering 1102 Everitt Laboratory, MC-278 1406 W. Green Street, University of Illinois at Urbana-Champaign, Urbana, 61801; Phone: (217) 300-0525; FAX: (217) 300-0525; email: jirudaya@illinois.edu

the most characterized epigenetic modification, involving multiple cellular processes. Generally, DNA methylation involves the transfer of a methyl group from the methyl donor S-adenosyl-L-methionine (SAM) to the C5 position of the cytosine in a CG dinucleotide to form 5-methylcytosine. During the cell cycle, DNA methylation is dynamically modified with DNA methyltransferase (DNMT) and ten-eleven translocation (TET) proteins. DNMTs (DNMT1, DNMT3A, DNMT3B) catalyze the transfer of a methyl group to the C5 cytosine [40]. DNMT1 functions to maintain the DNA methylation pattern after DNA replication by methylating the newly synthesized DNA strands using the parental strand DNA methylation pattern as a template [41]. DNMT3A and DNMT3B can methylate DNA de novo [42]. The methylated DNA could be chemically modified by TET proteins, which oxidizes the methyl group on the cytosine to form the hydroxymethyl group. DNMT and TET coregulate the dynamic state of DNA methylation, affecting the outcome of gene transcription.

To the best of our knowledge, the association of DEX with alteration in DNA methylation locally or globally has been well assessed for various clinical conditions, such as early life stress [43,44], congenital adrenal hyperplasia [45], and steroid-associated osteonecrosis [46]. However, the role of DEX in epigenetic regulation in ocular cells is not well understood. In this study, we aim to elucidate the potential molecular interactions between DEX and DNMT, underlying changes in global methylation induced with DEX.

In this work, we found that exposure to DEX induced global DNA hypomethylation and hyper-hydroxymethylation in ARPE-19 cells, but only hypomethylation in primary human RPE (hRPE) cells. Increased global DNA hydroxymethylation levels could be due to the upregulation of TET1–3 in ARPE-19 cells. Interestingly, DNMT1 and DNMT3B were upregulated, while DNMT3A is downregulated in ARPE-19 cells but not in hRPE cells. Moreover, we found that DEX could hinder the enzymatic activity of DNMT, specifically DNMT1. Together, we identified a potential mode of action of DEX in epigenetic alteration linked with DNMT and TET proteins.

METHODS

Cell culture: Adult human RPE cells were procured from ATCC (Manassas, VA; ARPE-19-CRL-2302™) authenticated with short tandem repeat (STR) analysis. Seventeen short tandem repeat (STR) loci plus the gender determining locus, Amelogenin, were amplified using the commercially available PowerPlex® 18D Kit from Promega (WI, Promega). The cell line sample was processed using the ABI Prism®

3500xl Genetic Analyzer. Data were analyzed using GeneMapper® ID-X v1.2 software (Applied Biosystems, Waltham, MA). Appropriate positive and negative controls were run and confirmed for each sample submitted. The STR analyses are presented in Appendix 1. While hRPE cells were a kind gift from Dr. S. Chidambaram [47]. Passages 4–8 and passages 3–6 of the ARPE-19 and hRPE cells were used for all experiments, respectively. Fifteen STR loci plus the gender-determining locus, amelogenin, were amplified using the commercially available PowerPlex 16 HS from Promega. The cell line sample was processed using the ABI Prism® 3500 Genetic Analyzer. Data were analyzed using GeneMapper® ID-X v1.5 software (Applied Biosystems). Appropriate positive and negative controls were run and confirmed for each sample submitted. The STR analyses are presented in Appendix 1. The cells were cultured in Dulbecco's Modified Eagle Medium/Ham's F-12 (1:1, DMEM/F-12, Corning, Corning, NY) supplemented with 10% fetal bovine serum (FBS, VWR, Radnor, PA), 100 IU/ml penicillin, and 100 mg/ml streptomycin at 37 °C in a 5% CO_2 incubator.

Chemicals: Dexamethasone (D4902, Sigma, 97%) was dissolved in dimethyl sulfoxide (DMSO), aliquot, and stored at −20 °C. Dexamethasone sodium phosphate (PHR1768, Sigma-Aldrich, St. Louis, MO) was dissolved in PBS (1X; 154 mM NaCl, 5.6 mM $NaPO_4$, 1 mM KH_2PO_4, pH 7.4) and stored at 4 °C.

MTT assay: 3-(4,5-dimethylthiazol-2-yl)-2,5-diphenyltetrazolium bromide (MTT) assay was performed as reported [48]. Briefly, approximately 8,000 ARPE-19 cells were added in each 96-well plate with DMEM/F-12, 10% FBS with antibiotics. After 24 h incubation, the cell culture medium was removed. Various amounts of DEX were added with fresh cell culture medium and incubated for 24 or 48 h. At the end of the treatment, 20 µl of MTT was added to each well from a 5 mg/ml stock in 1X PBS. The 96-well plates were incubated for 3.5 h at 37 °C. After incubation with MTT, the cell culture medium was removed carefully, and 150 µl of MTT solvent (4 mM HCl, 0.1 (v/v) % IGEPAL CA-630 in isopropanol) was added. After a 10 min incubation, a multipipettor was used to mix the wells before the absorbance was read at 570 nm. The background reading was subtracted from blank wells with MTT solvent. Within each experiment, drug treatments were conducted in quadruplicate, and the values were averaged.

Quantification of global DNA methylation and hydroxymethylation: Cells (about 10,000 cells/ml) were plated in T25 flasks for 24 h and then swapped with fresh cell culture medium with various amounts of DEX. After 48 h of incubation, cells were trypsinized for DNA extraction. Genomic DNA was extracted and purified with the PureLink Genomic

TABLE 1. PRIMER SEQUENCES FOR THE METHYLATION ENZYMES AND EPIGENETIC MARKS USED IN THIS STUDY.

S.No.	Gene name	Primer	Primer sequence
1	DNMT3A	FP	5'-TATTGATGAGCGCACAAGAGAGC −3'
		RP	5'-GGGTGTTCCAGGGTAACATTGAG-3'
2	DNMT3B	FP	5'-GGCAAGTTCTCCGAGGTCTCTG-3'
		RP	5'-TGGTACATGGCTTTTGGATAGGA-3'
3	DNMT1	FP	5'-TACCTGACGACCCTGACCTC-3'
		RP	5'-CGTTGGCATCAAAGATGGACA-3'
4	TET1	FP	5'-CAG AAC CTA AAC CAC CCG TG-3'
		RP	5'-TGC TTC GTA GCG CCA TTG TAA-3'
5	TET2	FP	5'-GAT AGA ACC AAC CAT GTT GAG GG-3'
		RP	5'-TGG AGC TTT GTA GCC AGA GGT-3'
6	TET3	FP	5'-TCC AGC AAC TCC TAG AAC TGA G-3'
		RP	5'-AGG CCG CTT GAA TAC TGA CTG-3'
7	MECP2	FP	5'-GTATTTGATCAATCCCCAGG −3'
		RP	5'-GTCAAAATCATTAGGGTCCAG-3'
8	MBD1	FP	5'-TGGTGATTCCAGCAAGTACAGA-3'
		RP	5'-CCACAGGCCAGGTTCTCAAT-3'
9	MBD3	FP	5'-GCCGGTGACCAAGATTACCA-3'
		RP	5'-ACCAGCTCCTCAGCAATGTC-3'
10	18s rRNA	FP	5′-AACCCGTTGAACCCCATT-3′
		RP	5′-CCATTCAATCGGTAGTAGCG-3′

DNA Mini Kit (Thermo Fisher Scientific, Waltham, MA) according to the manufacturer's instructions. The concentrations of extracted DNA were measured with a NanoDrop spectrophotometer (Thermo Fisher Scientific). The DNA methylation and hydroxymethylation levels were determined with the MethylFlash Global DNA methylation (5mC) enzyme-linked immunosorbent assay (ELISA) Easy Kit and the MethylFlash Global DNA Hydroxymethylation (5hmC) ELISA Easy Kit (EpiGentek, Farmingdale, NY) following the manufacturer's protocols.

Quantitative real-time PCR: ARPE-19/hRPE cells ($2*10^5$ cells/well) were seeded in six-well plates and serum-starved overnight using 1% FBS containing DMEM/F-12 medium. The following day, the cells were treated with 1 mg/ml and 2 mg/ml of dexamethasone sodium phosphate for 48 h. Total RNA was extracted using TRIzol reagent (Sigma Aldrich) and quantified using a NanoDrop spectrophotometer (Thermo Scientific). Further, 1 µg of the total RNA was used to synthesize cDNA (cDNA) using the iScript cDNA Conversion Kit (BioRad CFX96 Real-time system; Hercules, CA).

Quantitative real-time PCR (qRT-PCR) for the *DNMT1* (Gene ID: 1786, OMIM: 126375); *DNMT3A* (Gene ID: 1788, OMIM: 602769); *DNMT3B* (Gene ID: 1789, OMIM: 602900); *TET1* (Gene ID: 80312, OMIM:607790); *TET2* (Gene ID:

54790, OMIM: 612839); and *TET3* (Gene ID: 200424, OMIM: 613555) gene was performed with the primers listed in Table 1. qRT-PCR was performed with BioRad CFX96 Real-time system, initial denaturation at 95 °C for 10 min, followed by 40 cycles of denaturation at 95 °C for 15 s, annealing at 60 °C for 15 s and extension at 72 °C for 20 s. Samples were run in triplicates and the data were analyzed using the $2^{-\Delta\Delta ct}$ method after normalization with the housekeeping gene *18S rRNA*.

Evaluation of DNMT activities: To assess enzyme activity of overall human methyltransferases, we used the EpiQuik DNMT Activity/Inhibition Assay Ultra Kit (EpiGentek). The relative activity of overall DNMT was assayed with MU4 (DNMT positive control) provided by the kit, which is a mixture of purified human DNMT1, DNMT3A, and DNMT3B. Each condition was assayed twice, and the values were averaged. About 0.5 µg of DNMT positive control was used in each reaction well with 2.5 h reaction time. For quantification of DNMT1 activity, assays were performed similarly with 1.5 unit DNMT1 (NEB, M0230L) with 1.5 h reaction time. Relative DNMT activity was normalized against the reaction without adding DEX in each independent experiment.

Stimulated emission depletion microscopy: Stimulated emission depletion (STED) imaging, confocal imaging,

and fluorescence correlation spectroscopy (FCS) were performed with the Alba Imaging System (ISS, Champaign, IL). Details of the single-molecule instrumentation were described previously [48-51]. Samples were excited with a 640 nm picosecond laser, which was spatially and temporally coaligned with a circular-polarized donut-shaped 775 nm depletion beam (about 580 ps, NKT Photonics, Portland, OR) and combined with a 685 nm dichroic mirror (Chroma, Bellows Falls, VT). An apochromatic silicone oil objective collected emitted photons (100X, NA 1.35, Olympus, Shinjuku City, Japan). Photons were then filtered with a 780 nm long-pass filter (Chroma), a 640 nm bandpass filter (Chroma), a 50 µm pinhole, and a 679/41 emission filter (Chroma) before reaching the avalanche photodiode SPCM-AQRH-15 (Excelitas, Waltham, MA; pixel size 23.4 nm). Deconvolution of STED images was performed with Huygens Essential (SVI, Hilversum, Netherlands) described previously [50] and similarly in the literature [52].

Image analysis: 5hmC cluster analysis was performed with CellProfiler is free, open-source software license (BSD-3 clause) [53]. 5hmC clusters were thresholded with the Otsu three-class method and then segmented based on intensity distributions. Then cluster morphology, neighbors, and intensity distribution were estimated accordingly and summarized in Appendix 2. To quantify single-cell morphological features with phenotype analysis, principal component analysis (PCA) and *t*-distributed stochastic neighbor embedding (*t*-SNE) with the Barnes-Hut approximation (30 perplexities) were performed using BioVinci software (BioTuring, San Diego, CA, Version 3.0.9).

Statistical analysis: For the MTT, qRT-PCR, and ELISA data, the Student *t* test was used to test the statistical significance of the sample populations (significance level is α= 0.05). For the 5hmC image analysis, the Mann–Whitney test was used.

Immunofluorescence staining: Around 10,000 ARPE-19 cells were seeded on round 18-mm, No 1.5H coverslips (Azer Scientific, Morgantown, PA). The coverslips were coated with poly-L-lysine (Sigma) in 12-well plates under ultraviolet (UV) light and rinsed at least three times with sterile Milli-Q water. After 24 h of incubation, various concentrations of DEX were added and incubated for 48 h. The cells were then fixed with ice-cold 4% paraformaldehyde for 10 min and rinsed with 1X PBS. Cell membrane was permeabilized with 0.3% Triton-X for 20 min and then rinsed with 1X PBS. The DNA denaturation step was performed with 1 M HCl for 30 min and neutralized with 100 mM Tris-HCl (pH 8). The cells were further washed with 1X PBS three times. After PBS washing, the cells were blocked with 1% bovine serum albumin (BSA) for 45 min. The 5hmC antibody (Active Motif, 39,069, 1:250)

was diluted in 1X PBS containing 0.5% BSA and then added to each sample and incubated in a humid chamber at 4 °C overnight. The cells were then rinsed three times with 1X PBS containing 0.01% Tween-20 before being incubated with goat anti-rabbit Atto647N for 2 h. The samples were then rinsed with 1X PBS before transfer to the imaging chamber.

RESULTS

DEX induced global DNA hypomethylation and hyperhydroxymethylation: Under tested concentrations of dexamethasone exposure, we found that ARPE-19 cells are highly sensitive to DMSO exposure (Appendix 3) as well as changes in the 5mC level in as low as 0.2% DMSO (data not shown). DMSO is known to alter DNA methylation via different mechanisms [54-56]. To rule out the intermix effect of DMSO, we selected DEX for exposure [57,58]. DEX is water-soluble at physiologic pH in dianionic form and could rapidly convert into dexamethasone in organisms [59].

First, the effect of dexamethasone sodium phosphate on cell cytotoxicity was examined with MTT assay as shown in Figure 1A. We did not observe changes in relative cell viability upon exposure to DEX at up to the 3.5 mg/ml exposure level (Appendix 4). Next, the global methylation and hydroxymethylation levels of genomic DNA were quantified with a fluorescence-based ELISA, and the results are summarized in Figure 1B, C. Exposure of DEX at 2 mg/ml caused significant reduction in global DNA methylation. Compared with the control group, 1 mg/ml DEX exposure led to an average of about 21% reduction in the DNA methylation level, whereas 2 mg/ml DEX exposure resulted in an average reduction of about 42%. However, the global DNA hydroxymethylation level increased at higher exposure levels. Compared with the control group, 1 mg/ml of DEX exposure induced about a 41% increase in the DNA hydroxymethylation level and about a 2.1-fold increase at the 2 mg/ml DEX exposure.

DEX altered DNMT and TET expression patterns: To investigate the mechanism underlying DNA methylation and hydroxymethylation changes induced by DEX, we evaluated the expression level of DNMTs and TETs with qRT-PCR as shown in Figure 2. We found that the expression level of DNMT1 and DNMT3B was significantly elevated at 2 mg/ml and 1 mg/ml of DEX exposure, respectively, whereas the expression level of DNMT3A was significantly reduced under the tested conditions. TET1 and TET3 were significantly upregulated under 2 mg/ml of exposure to DEX, whereas TET2 was mildly upregulated. This is consistent with the observed elevated levels of 5-hydroxymethylation, suggesting DEX induced epigenetic changes associated with DNMTs and TETs. Additionally, we did not observe significant changes in
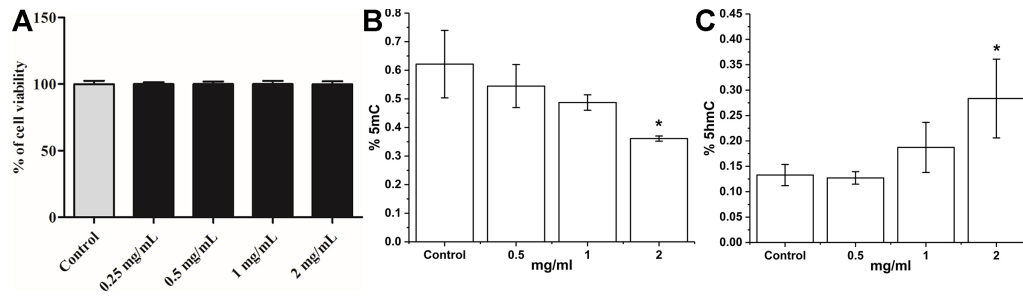
Figure 1. DEX exposure induces alteration in DNA methylation and hydroxymethylation. **A**: 3-(4,5-dimethylthiazol-2-yl)-2,5-diphenyltet-razolium bromide (MTT) assay was performed after 48 h of incubation at various concentrations of dexamethasone (DEX). No significant changes in cell viability were observed. **B**: Changes in the genomic DNA methylation level of ARPE-19 cells exposed to 0.5, 1.0, and 2.0 mg/ml DEX after 48 h. **C**: Changes in the genomic DNA hydroxymethylation level of ARPE-19 cells exposed to 0.5, 1.0, and 2.0 mg/ml of DEX after 48 h. *p<0.05 with the Student two-tailed *t* test compared to the control group. n=3.

methyl-binding-domain proteins, specifically methyl-CpG-binding domain protein 1, 3, and methyl-CpG-binding protein 2 (Appendix 5).

DEX inhibited the activity of DNMTs: Intriguingly, even with an elevated level of DNMT1 and DNMT3B, DEX unexpect-edly induced global hypomethylation. To this end, we evalu-ated the effect of DEX on the DNMT catalyzed reaction in vitro. We hypothesized that DEX may play a direct role in the formation of 5mC through DNMTs. The relative activity of DNMT under DEX exposure was evaluated with a colori-metric ELISA-based assay. The relative overall activity of the DNMTs was significantly reduced by DEX beyond 1 mg/ml exposure, with a reduction to 62±12% at 1 mg/ml exposure and further reduced to 47±8.0% at 2 mg/ml exposure (Figure 3A). The activity of DNMT1 was also reduced to about 67% and 57%, with 1 mg/ml and 2 mg/ml of DEX exposure, respectively (Figure 3B).

STED revealed 5hmC nanocluster alterations upon DEX exposure: Although DNA 5mC and 5hmC are affected by DEX exposure, current literature indicates that TET1/3 associated epigenetic alteration focused on 5hmC by DEX [46,60,61]. We asked whether DEX exposure could alter the 5hmC pattern using super-resolution microscopy (STED). Typical immunostaining of 5hmC in ARPE-19 cells is shown in Figure 4A upon exposure to DEX as shown in Figure 4B, C. Image analysis was performed with CellProfiler to segment single 5hmC nanoclusters (Appendix 6). We first quantified the number of 5hmC nanoclusters (Figure 4B) and observed that under 1 mg/ml DEX exposure, there is a significant reduction of 5hmC nanoclusters, whereas 2 mg/ml DEX exposure showed similar nanocluster counts compared to the control cells. Next, we determined the size distribution of 5hmC clusters in the nuclei and found that upon DEX exposure (Figure 4C), the 5hmC nanoclusters displayed increased size (averaged control nanoclusters: 20
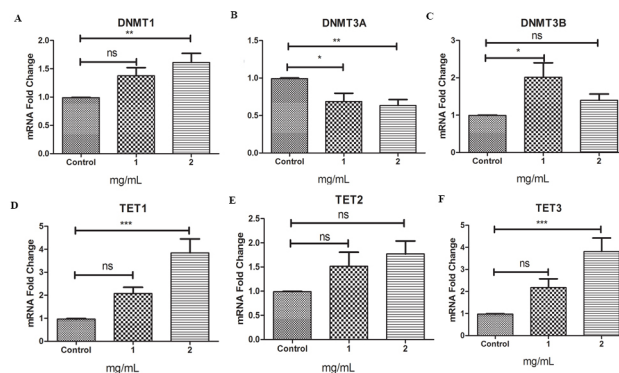

Figure 2. DEX exposure alters mRNA expression levels of DNMTs and TETs. The transcription level of DNA methylation-related enzymes, DNA methyltransferases (DNMTs) (**A–C**), and ten-eleven translocations (TETs) (**D–F**) was determined with quantitative real-time PCR (qRT-PCR) after 48 h of dexamethasone (DEX) exposure. Data from three independent experiments (mean ± standard deviation [SD]).*p<0.05, **p<0.01, ***p<0.001 with the Student two-tailed *t* test.
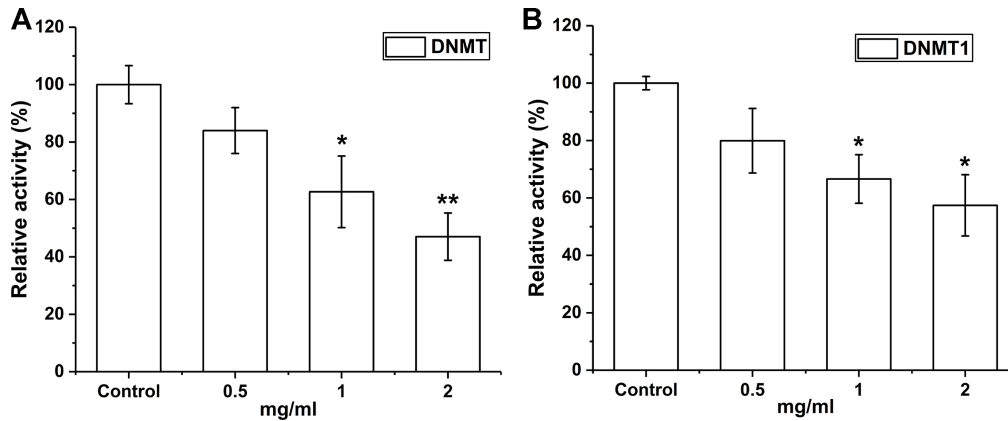
Figure 3. DEX exposure reduces DNMT enzymatic activity in vitro. Relative enzymatic activity of (**A**) DNA methyltransferases (DNMTs) and (**B**) DNMT1 from purified human DNMTs. Upon dexamethasone (DEX) exposure, the activity of the DNMTs was inhibited. (Data are shown as mean ± standard deviation [SD] from three independent experiments.) *p<0.05, **p<0.005 with the Student two-tailed *t* test.

$\times 10^3$ nm²; 1 mg/ml: 20.7×10^3 nm²; 2 mg/ml: 23.9×10^3 nm²) indicating the increased formation of larger kilobase-nano-clusters [62]. We further computed the cluster first nearest neighbor distance (NND, centroid to centroid) to evaluate the spatial organization of the 5hmC nanoclusters and found similar distribution among the three groups (Figure 4D). We assessed the spatial distribution of 5hmC in the nuclei with its intensity distribution relative to the centroid of the nucleus. The normalized 5hmC intensity distribution in Figure 4E shows increased nanocluster formation near the peripheral region of the nucleus. It does not show any significant difference between control and cells exposed to DEX, suggesting that DEX exposure does not induce noticeable chromatin organization alterations. Last, we wondered whether DEX exposure induces a phenotypical 5hmC pattern from an imaging perspective. To this end, we analyzed the averaged 5hmC nanocluster parameters in each nucleus among the control, 1 mg/ml, and 2 mg/ml DEX exposure with *t*-SNE shown in Figure 4F. We observed that the ensemble nucleus 5hmC features were separated into six different groups, with distinct clusters between the control and 2 mg/ml DEX exposure shown in Figure 4G. Together, the results reveal an altered 5hmC pattern upon exposure to DEX.

DEX induced global DNA hypomethylation in hRPE cells: We further quantified epigenetic changes upon exposure to DEX in hRPE cells. The global methylation level of genomic DNA was quantified and is shown in Figure 5A. We observed significantly reduced 5mC levels at 1 mg/ml and 2 mg/ml DEX exposure, exhibiting DEX-induced global hypomethylation. Upon evaluating the expression level of the DNMTs (Figure 5B–D), we found that the expression level of DNMT3A was significantly reduced under 1 mg/ml DEX. DNMT1 and DNMT3B were not affected, suggesting the

possibility of global hypomethylation due to DEX inhibition of DNMT enzymatic activities. We then quantified the global hydroxymethylation level in hRPE cells (Figure 5E) as well as the expression level of TETs (Figure 5F–H). Unlike the ARPE-19 cells, under the tested condition, the impact of DEX on hydroxymethylation was not significantly altered.

DISCUSSION

In this study, we evaluated the effects of exposure to DEX on DNA methylation and hydroxymethylation at the molecular scale. For the DEX exposure levels used in the ARPE-19 cells, no significant cell viability changes were observed, but the expression levels of DNMT1, DNMT3A, DNMT3B, TET1, and TET3 were affected and found to be associated with changes in DNA methylation and hydroxymethylation globally, providing novel insights into how DEX mediates epigenetic alterations by modulating the expression and activity of the DNMT and TET enzymes. Consistent with the literature, downregulation of DNMT3A and upregulation of TET3 were reported for the embryonic neural stem cell model [60]. However, upregulated DNMT1 and DNMT3B were not reported previously, providing contradictory evidence of DEX-induced DNA hypomethylation. To resolve this discrepancy, we examined the effect of DEX on DNA hypomethylation. A previous study indicated that DEX could induce conformational change of a complex involving GR, and MeCP2, as well as recruitment of DNMT3B [63]. The recruitment of DNMT3B potentially hints that it is possible for DEX to act directly with DNMTs, considering that DNMT3B cooperates with DNMT3L to contribute to the methylation of DNA by a non-cooperative mechanism [64,65]. We wondered whether alterations in DNA methylation could be a result of direct interaction between DEX and

DNMT. To test this hypothesis, we assessed the enzymatic activity of DNMTs to methylate DNA in vitro. We discovered that DEX could inhibit the overall enzymatic activity of DNMTs. Specifically, the activity of DNMT1 was significantly hindered by DEX. As expected, the upregulation of

TET1 and TET3 is consistent with the observed global DNA hyper-hydroxymethylation.

We further investigated the distribution of 5hmC in ARPE-19 cells with STED microscopy and analyzed the nuclear localization patterns of 5hmC upon DEX exposure. The number of 5hmC clusters at the 1 mg/ml DEX
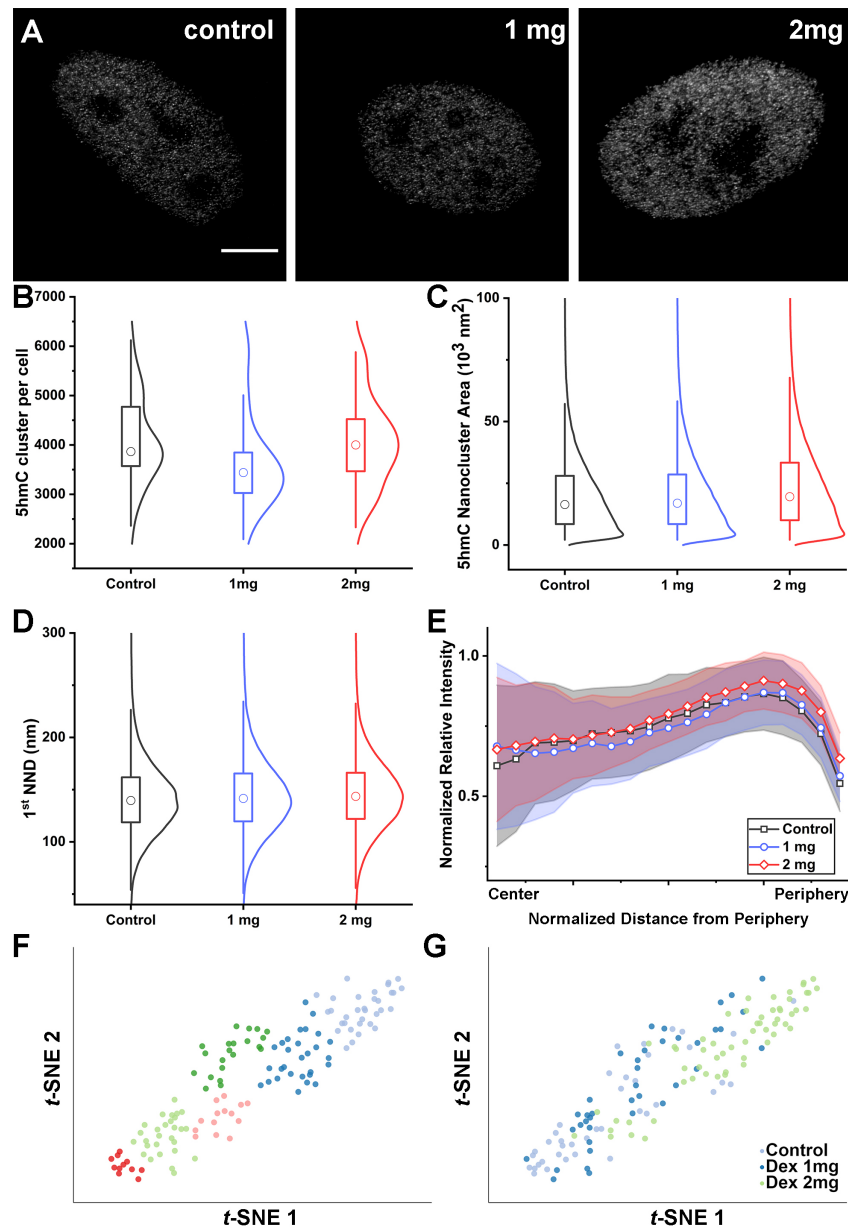

Figure 4. DEX exposure induces changes in global 5hmC structures. Typical stimulated emission depletion (STED) image of the 5hmC pattern in (**A**) control, 1 mg/ml dexamethasone (DEX), and 2 mg/ml DEX after 48 h. **B**: 5hmC cluster number distribution per cell nucleus. *p<0.01 with the Mann–Whitney test. **C**: Violin plot of the 5hmC cluster area. **D**: 5hmC nearest neighbor distance (NND) distribution. **E**: The 5hmC density distribution is shown versus the normalized distance from the nucleus center position with 20 radial rings. **F**: *t*-distributed stochastic neighbor embedding (*t*-SNE) analysis of the average 5hmC cluster features in each nucleus. **G**: *t*-SNE analysis of the grouped 5hmC cluster features in the control, 1 mg/ml DEX, and 2 mg/ml DEX after 48 h. Violin plots are shown with 25%, median (round mark), 75%, smooth kernel curve. Data collected from 40 to 60 cells in three experiments.

exposure significantly decreased, while the global 5hmC level increased as noted from the ELISA-based measurements. This could have resulted in an increased 5hmC nanocluster size and intensity, contributing to an overall increase in the 5hmC level with a decrease in the 5hmC nanocluster counts. We discovered that under 2 mg/ml DEX exposure, the 5hmC pattern generates significant alteration evaluated with *t*-SNE, suggesting the possible indication of 5hmC changes upon DEX exposure. Such changes could be influenced by DEX on cell cycle–induced reorganization of the chromatin, and could be further explored with sequencing techniques [66]. Others have shown that the dynamic patterns of DNMTs and the correlation with the 5mC and 5hmC pattern could be an indication of the chromatin remodeling during retinogenesis, which may be further explored [67-70].

Apart from molecular interactions of DEX, other factors could also trigger epigenetic alterations. Dexamethasone is known to trigger oxidative stress [71-74], and oxidative stress has been implicated in epigenetic alterations [75]. The elevated reactive oxygen species (ROS) could result in increased metabolic activity, mitochondrial dysfunction, and increased activity of peroxisome and oxidases, among others. Elevated ROS have been associated with global hypomethylation or hypermethylation in different models [76,77], where the role of oxidative stress in TM cells and retinal cells is associated with a disease state such as glaucoma [78-80].

Although ARPE-19 cells provide a dependable and widely used alternative to native RPE cells, they tend to lose RPE phenotypes after multiple passages [81,82]. RPE cells can initiate proliferation once reverted to a more immature state by partial demethylation of the genome [83]. RPE cell proliferation could be activated into disease states, with association with epithelial to mesenchymal transition, growth of epiretinal membranes [84], and choroidal tumors [85]. To this end, we tested DEX exposure in human RPE cells (Figure 5). As expected, we observed hypomethylation in human RPE cells (Figure 5A). Alteration in the 5mC pattern could be explained by changes in DNMT activities without alteration in the DNMT expression level. Unexpectedly, the 5hmC pattern was significantly different from that in ARPE-19 cells (Figure 5E–H), which requires further exploration in the future. Consistent with ARPE-19 cell data, others have shown that dexamethasone plays a role in TET1/TET3-mediated epigenetic alterations in multiple cell models from patients as well as mice models [46,60,61,86]. These results in hRPE cells were somewhat surprising, and the role of 5hmC and TET in ocular cells remains open for further investigation in the field. In this report, we elucidated alterations in DNA methylation induced by DEX due to changes in the expression of DNMTs and TETs. Additionally, DEX-induced DNA hypomethylation could be a direct result of the action of DEX on DNMT, providing new mechanistic insights into the effect of DEX on ocular diseases.

Corticosteroids in any form (for ocular-topical and intravitreal, skin application, systemic) have been shown to cause steroid-induced ocular hypertension or glaucoma
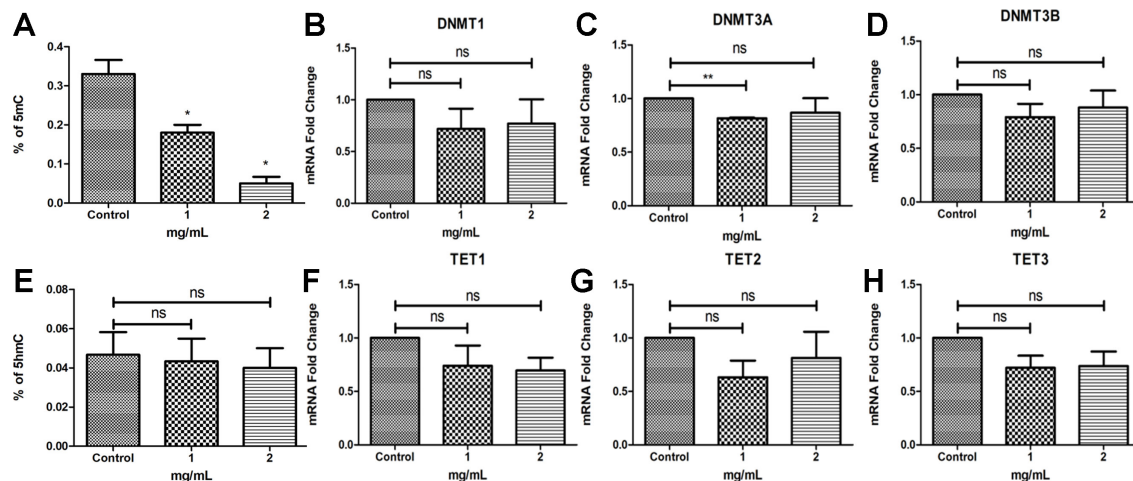

Figure 5. DEX exposure induces alteration in DNA methylation in hRPE cells. **A**: Changes in the genomic DNA methylation level of human RPE (hRPE) cells exposed to 1 mg/ml and 2 mg/ml dexamethasone (DEX) after 48 h. The transcription level of the DNA methyltransferases (DNMTs) (**B**–**D**) was determined with quantitative real-time PCR (qRT-PCR) after 48 h of DEX exposure. **E**: Changes in the genomic DNA hydroxymethylation level of the hRPE cells exposed to 1 mg/ml and 2 mg/ml of DEX after 48 h. The transcription levels of ten-eleven translocations (TETs) (**F**–**H**) were determined with qRT-PCR after 48 h of DEX exposure. *$p<0.05$, **$p<0.005$ with the Student two-tailed *t* test compared to the control group. n=3.

(SIG) in susceptible individuals [87]. Intravitreal corticosteroid treatment for certain ocular conditions, such as diabetic macular edema (DME), retinal vein occlusion (RVO), and inflammatory conditions with cystoid macular edema, cause an increase in IOP in approximately 58.3% of patients with existing glaucomatous changes [88] and in 20%–30% of patients with no previous history or risk factors for glaucoma. Epigenome is increasingly associated with several ocular diseases, such as cataracts, ocular surface disorders, and glaucoma [89,90]. One study on SIG implicated altered DNA methylation regulating the expression of several genes in DEX-treated primary TM cells [91].

Further, although a combined treatment regime of immunosuppressive drugs with corticosteroids is prescribed as long-term therapy in managing ocular inflammation [92], detrimental side effects with retinal degenerative changes in the rat animal model have been reported [93]. However, immunosuppressive action of dexamethasone was crucial toward successful differentiation and survival of retinal organoids following epiretinal transplantation [15]. The conflicting reports can be attributed to the dosage, exposure, and responsiveness of specific immune cell types upon DEX treatment thus warranting caution in long-term prescription of these drugs in clinical settings. For instance, evidence indicates that DEX could also have a stimulating effect on immune cells, such as macrophages and regulatory T cells (Tregs), by upregulation of FOX3P expression [94,95]. Further, deletion of DNMT1 in conventional T cells increases FOX3p stimulation upon TCR stimulation promoting their conversion to induced Tregs cells [96]. However, deletion of DNMT1 in natural Treg cells altered Tregs transcriptional activity that can lead to lethal autoimmunity [96]. Thus, epigenetic regulation of specific immune response cells upon acute and chronic DEX treatment in target tissues with implications in ocular pathology must be considered and patients closely monitored for adverse effects of the drugs.

As epigenetic mechanisms are increasingly associated with efficacy of immunotherapy [97], delineating its kinetics would be useful toward developing a clinical regime especially with other drugs in treating ocular disorders. Understanding the role of epigenome and its regulation will provide an exciting window of opportunity for developing therapeutic targets for ocular diseases dependent on corticosteroid treatments.

APPENDIX 1. STR ANALYSIS.

To access the data, click or select the words "Appendix 1."

APPENDIX 2. SUPPLEMENTARY TABLE 1.

To access the data, click or select the words "Appendix 2."

APPENDIX 3. SUPPLEMENTARY FIGURE 1.

To access the data, click or select the words "Appendix 3."

APPENDIX 4. SUPPLEMENTARY FIGURE 2.

To access the data, click or select the words "Appendix 4."

APPENDIX 5. SUPPLEMENTARY FIGURE 3.

To access the data, click or select the words "Appendix 5."

APPENDIX 6. SUPPLEMENTARY FIGURE 4.

To access the data, click or select the words "Appendix 6."

ACKNOWLEDGMENTS

REFERENCES

1. Teja S, Sawatzky L, Wiens T, Maberley D, Ma P. Ozurdex for refractory macular edema secondary to diabetes, vein occlusion, uveitis and pseudophakia. Can J Ophthalmol 2019; 54:540-7. [PMID: 31564342].

2. Benhamou N, Massin P, Haouchine B, Audren F, Tadayoni R, Gaudric A. Intravitreal triamcinolone for refractory pseudophakic macular edema. Am J Ophthalmol 2003; 135:246-9. [PMID: 12566041].

3. Spaide RF, Sorenson J, Maranan L. Combined photodynamic therapy and intravitreal triamcinolone for nonsubfoveal choroidal neovascularization. Retina 2005; 25:685-90. [PMID: 16141854].

4. Spaide RF, Sorenson J, Maranan L. Photodynamic therapy with verteporfin combined with intravitreal injection of triamcinolone acetonide for choroidal neovascularization. Ophthalmology 2005; 112:301-4. [PMID: 15691567].

5. Kok H, Lau C, Maycock N, McCluskey P, Lightman S. Outcome of intravitreal triamcinolone in uveitis. Ophthalmology 2005; 112:1916.e1-7. [PMID: 16171868].

6. Lashay A, Riazi-Esfahani H, Mirghorbani M, Yaseri M. Intravitreal Medications for Retinal Vein Occlusion: Systematic Review and Meta-analysis. J Ophthalmic Vis Res 2019; 14:336-66. [PMID: 31660113].

7. Martidis A, Duker JS, Greenberg PB, Rogers AH, Puliafito CA, Reichel E, Baumal C. Intravitreal triamcinolone for refractory diabetic macular edema. Ophthalmology 2002; 109:920-7. [PMID: 11986098].

8. Altintas AGK, Ilhan C. Intravitreal Dexamethasone Implantation in Intravitreal Bevacizumab Treatment-resistant Pseudophakic Cystoid Macular Edema. Korean J Ophthalmol 2019; 33:259-66. [PMID: 31179657].

9. Ip MS, Gottlieb JL, Kahana A, Scott IU, Altaweel MM, Blodi BA, Gangnon RE, Puliafito CA. Intravitreal Triamcinolone for the Treatment of Macular Edema AssociatedWith Central Retinal Vein Occlusion. JAMA Ophthalmol 2004; 122:1131-6. [PMID: 15302652].

10. Edelman JL. Differentiating Intraocular Glucocorticoids. Ophthalmologica 2010; 224:25-30. .

11. Ioannis T, Chryssanthi K, Dimitrios P, Theodore P, Ilias G. Safety and Efficacy of Dexamethasone Intravitreal Implant (Ozurdex) for the Treatment of Persistent Macular Edema Secondary to Retinal Vein Occlusion in Eyes Previously Treated with Anti-Vascular Endothelial Growth Factors. Curr Drug Saf 2015; 10:145-51. [PMID: 25092480].

12. Sarda V, Fajnkuchen F, Nghiem-Buffet S, Grenet T, Chaine G, Giocanti-Auregan A. Efficacité précoce de l'implant de dexaméthasone (OZURDEX®) évaluée en vraie vie dans le traitement de l'œdème maculaire diabétique. J Fr Ophtalmol 2017; 40:408-13. [PMID: 28336283].

13. Boyer DS, Yoon YH, Belfort R Jr, Bandello F, Maturi RK, Augustin AJ, Li X-Y, Cui H, Hashad Y, Whitcup SM. Three-Year, Randomized, Sham-Controlled Trial of Dexamethasone Intravitreal Implant in Patients with Diabetic Macular Edema. Ophthalmology 2014; 121:1904-14. [PMID: 24907062].

14. Haller JA, Bandello F, Belfort R Jr, Blumenkranz MS, Gillies M, Heier J, Loewenstein A, Yoon YH, Jiao J, Li X-Y, Whitcup SM. Dexamethasone Intravitreal Implant in Patients with Macular Edema Related to Branch or Central Retinal Vein Occlusion: Twelve-Month Study Results. Ophthalmology 2011; 118:2453-60. [PMID: 21764136].

15. Xian B, Luo Z, Li K, Li K, Tang M, Yang R, Lu S, Zhang H, Ge J. Dexamethasone Provides Effective Immunosuppression for Improved Survival of Retinal Organoids after Epiretinal Transplantation. Stem Cells Int 2019; 2019:7148032-[PMID: 31428159].

16. Chang Y-C, Wu W-C. Elevation of intraocular pressure after intravitreal injection of triamcinolone acetonide in Taiwanese patients. Kaohsiung J Med Sci 2008; 24:72-7. [PMID: 18281223].

17. Wannamaker KW, Kenny S, Das R, Mendlovitz A, Comstock JM, Chu ER, Bahadorani S, Gresores NJ, Beck KD, Krambeer CJ, Kermany DS, Diaz-Rohena R, Nolan DP, Sohn J-H, Singer MA. The effects of temporary intraocular pressure spikes after intravitreal dexamethasone implantation on the retinal nerve fiber layer. Clin Ophthalmol 2019; 13:1079-86. [PMID: 31417237].

18. Hasanreisoğlu M, Özdemir HB, Özkan K, Yüksel M, Aktaş Z, Atalay HT, Özdek Ş, Gürelik G. Intravitreal Dexamethasone Implant in the Treatment of Non-infectious Uveitis. Turk J Ophthalmol 2019; 49:250-7. [PMID: 31650791].

19. Alba-Linero C, Sala-Puigdollers A, Romero B, Llorenç V, Adan A, Zarranz-Ventura J. Long-Term Intravitreal Dexamethasone Implant Outcomes in Uveitis. Ocul Immunol Inflamm 2019; 10:228-237. [PMID: 30994370].

20. Sharif F, Steenbergen PJ, Metz JR, Champagne DL. Long-lasting effects of dexamethasone on immune cells and wound healing in the zebrafish. Wound Repair Regen 2015; 23:855-65. .

21. Morgan DJ, Davis DM. Distinct Effects of Dexamethasone on Human Natural Killer Cell Responses Dependent on Cytokines. Front Immunol 2017; 8:432-[PMID: 28450865].

22. Moisseiev E, Goldstein M, Waisbourd M, Barak A, Loewenstein A. Long-term evaluation of patients treated with dexamethasone intravitreal implant for macular edema due to retinal vein occlusion. Eye (Lond) 2013; 27:65-71. [PMID: 23154502].

23. Timmermans S, Souffriau J, Libert C. A General Introduction to Glucocorticoid Biology. Front Immunol 2019; 10:1545-[PMID: 31333672].

24. Steely HT, Browder SL, Julian MB, Miggans ST, Wilson KL, Clark AF. The effects of dexamethasone on fibronectin expression in cultured human trabecular meshwork cells. Invest Ophthalmol Vis Sci 1992; 33:2242-50. [PMID: 1607235].

25. Snyder RW, Stamer WD, Kramer TR, Seftor RE. Corticosteroid treatment and trabecular meshwork proteases in cell and organ culture supernatants. Exp Eye Res 1993; 57:461-8. [PMID: 8282032].

26. Samples JR, Alexander JP, Acott TS. Regulation of the levels of human trabecular matrix metalloproteinases and inhibitor by interleukin-1 and dexamethasone. Invest Ophthalmol Vis Sci 1993; 34:3386-95. [PMID: 8225873].

27. Clark AF, Wilson K, McCartney MD, Miggans ST, Kunkle M, Howe W. Glucocorticoid-induced formation of cross-linked actin networks in cultured human trabecular meshwork cells. Invest Ophthalmol Vis Sci 1994; 35:281-94. [PMID: 8300356].

28. Sun YY, Bradley JM, Keller KE. Phenotypic and Functional Alterations in Tunneling Nanotubes Formed by Glaucomatous Trabecular Meshwork Cells. Invest Ophthalmol Vis Sci 2019; 60:4583-95. [PMID: 31675075].

29. Tripathi BJ, Tripathi RC, Swift HH. Hydrocortisone-induced DNA endoreplication in human trabecular cells in vitro. Exp Eye Res 1989; 49:259-70. [PMID: 2767172].

30. Matsumoto Y, Johnson DH. Dexamethasone decreases phagocytosis by human trabecular meshwork cells in situ. Invest Ophthalmol Vis Sci 1997; 38:1902-7. [PMID: 9286282].

31. Rashid JR, Spengler RF, Wagner RM, Melanson C, Skillen EL, Mays RA Jr, Heurtin-Roberts S, Long JA. Eliminating health disparities through transdisciplinary research, cross-agency

collaboration, and public participation. Am J Public Health 2009; 99:1955-61. [PMID: 19762652].

32. Raffaele N, Marchese A, Ghigo D. Compared antioxidant activity among corticosteroids on cultured retinal pigment epithelial cells. Graefes Arch Clin Exp Ophthalmol 2016; 254:2411-6. [PMID: 27743160].

33. Pereiro X, Ruzafa N, Acera A, Fonollosa A, Rodriguez FD, Vecino E. Dexamethasone protects retinal ganglion cells but not Müller glia against hyperglycemia in vitro. PLoS One 2018; 13:e0207913-.

34. Karlsson L, Barbaro M, Ewing E, Gomez-Cabrero D, Lajic S. Epigenetic Alterations Associated With Early Prenatal Dexamethasone Treatment. J Endocr Soc 2018; 3:250-63. [PMID: 30623163].

35. Cartier J, Smith T, Thomson JP, Rose CM, Khulan B, Heger A, Meehan RR, Drake AJ. Investigation into the role of the germline epigenome in the transmission of glucocorticoid-programmed effects across generations. Genome Biol 2018; 19:50-[PMID: 29636086].

36. Razin A, Riggs AD. DNA methylation and gene function. Science 1980; 210:604-[PMID: 6254144].

37. Yang Y, Hsu PJ, Chen Y-S, Yang Y-G. Dynamic transcriptomic m6A decoration: writers, erasers, readers and functions in RNA metabolism. Cell Res 2018; 28:616-24. [PMID: 29789545].

38. Bannister AJ, Kouzarides T. Regulation of chromatin by histone modifications. Cell Res 2011; 21:381-95. [PMID: 21321607].

39. Makunin IV, Mattick JS. Non-coding RNA. Hum Mol Genet 2006; 15:R17-29. .

40. El-Osta A. DNMT cooperativity—the developing links between methylation, chromatin structure and cancer. BioEssays 2003; 25:1071-84. [PMID: 14579248].

41. Robert M-F, Morin S, Beaulieu N, Gauthier F, Chute IC, Barsalou A, MacLeod AR. DNMT1 is required to maintain CpG methylation and aberrant gene silencing in human cancer cells. Nat Genet 2003; 33:61-[PMID: 12496760].

42. Lei H, Oh SP, Okano M, Juttermann R, Goss KA, Jaenisch R, Li E. De novo DNA cytosine methyltransferase activities in mouse embryonic stem cells. Development 1996; 122:3195-[PMID: 8898232].

43. Wiechmann T, Röh S, Sauer S, Czamara D, Arloth J, Ködel M, Beintner M, Knop L, Menke A, Binder EB, Provençal N. Identification of dynamic glucocorticoid-induced methylation changes at the FKBP5 locus. Clin Epigenetics 2019; 11:83-[PMID: 31122292].

44. Braun PR, Tanaka-Sahker M, Chan AC, Jellison SS, Klisares MJ, Hing BW, Shabbir Y, Gaul LN, Nagahama Y, Robles J, Heinzman JT, Sabbagh S, Cramer EM, Duncan GN, Yuki K, Close LN, Dlouhy BJ, Howard Iii MA, Kawasaki H, Stein KM, Potash JB, Shinozaki G. Genome-wide DNA methylation investigation of glucocorticoid exposure within buccal samples. Psychiatry Clin Neurosci 2019; 73:323-30. [PMID: 30821055].

45. Karlsson L, Barbaro M, Ewing E, Gomez-Cabrero D, Lajic S. Epigenetic Alterations Associated With Early Prenatal Dexamethasone Treatment. J Endocr Soc 2018; 3:250-63. [PMID: 30623163].

46. Zhao J, Ma X-l, Ma J-x, Sun L, Lu B, Wang Y, Xing G-s, Wang Y, Dong B-c, Xu L-y, Kuang M-J, Fu L, Bai H-h, Ma Y, Jin W-l. TET3 Mediates Alterations in the Epigenetic Marker 5hmC and Akt pathway in Steroid-Associated Osteonecrosis. J Bone Miner Res 2017; 32:319-32. [PMID: 27627619].

47. Palanisamy K, Karunakaran C, Raman R, Chidambaram S. Optimization of an in vitro bilayer model for studying the functional interplay between human primary retinal pigment epithelial and choroidal endothelial cells isolated from donor eyes. BMC Res Notes 2019; 12:307-[PMID: 31146784].

48. Liu W, Cui Y, Ren W, Irudayaraj J. Epigenetic biomarker screening by FLIM-FRET for combination therapy in ER+ breast cancer. Clin Epigenetics 2019; 11:16-[PMID: 30700309].

49. Liu W, Biton E, Pathania A, Matityahu A, Irudayaraj J, Onn I. Monomeric cohesin state revealed by live-cell single-molecule spectroscopy. EMBO Rep 2020; 21:e48211-[PMID: 31886609].

50. Liu W, Irudayaraj J. Perfluorooctanoic acid (PFOA) exposure inhibits DNA methyltransferase activities and alters constitutive heterochromatin organization. Food Chem Toxicol 2020; 141:111358-[PMID: 32315686].

51. Pathania A, Liu W, Matityahu A, Irudayaraj J, Onn I. Chromosome loading of cohesin depends on conserved residues in Scc3. Curr Genet 2021; 67:447-459. [PMID: 33404730].

52. Li H, Yang J, Tian C, Diao M, Wang Q, Zhao S, Li S, Tan F, Hua T, Qin Y, Lin C-P, Deska-Gauthier D, Thompson GJ, Zhang Y, Shui W, Liu Z-J, Wang T, Zhong G. Organized cannabinoid receptor distribution in neurons revealed by super-resolution fluorescence imaging. Nat Commun 2020; 11:5699-[PMID: 33177502].

53. Carpenter AE, Jones TR, Lamprecht MR, Clarke C, Kang IH, Friman O, Guertin DA, Chang JH, Lindquist RA, Moffat J, Golland P, Sabatini DM. CellProfiler: image analysis software for identifying and quantifying cell phenotypes. Genome Biol 2006; 7:R100-[PMID: 17076895].

54. Kawai K, Li Y-S, Song M-F, Kasai H. DNA methylation by dimethyl sulfoxide and methionine sulfoxide triggered by hydroxyl radical and implications for epigenetic modifications. Bioorg Med Chem Lett 2010; 20:260-5. [PMID: 19914833].

55. Thaler R, Spitzer S, Karlic H, Klaushofer K, Varga F. DMSO is a strong inducer of DNA hydroxymethylation in preosteoblastic MC3T3–E1 cells. Epigenetics 2012; 7:635-51. [PMID: 22507896].

56. Iwatani M, Ikegami K, Kremenska Y, Hattori N, Tanaka S, Yagi S, Shiota K. Dimethyl Sulfoxide Has an Impact on Epigenetic Profile in Mouse Embryoid Body. Stem Cells 2006; 24:2549-56. [PMID: 16840553].

57. Samtani MN, Jusko WJ. Stability of dexamethasone sodium phosphate in rat plasma. Int J Pharm 2005; 301:262-6. [PMID: 16054309].

58. Hao H-x, Wang J-k, Wang Y-l. Solubility of Dexamethasone Sodium Phosphate in Different Solvents. J Chem Eng Data 2004; 49:1697-8. .

59. Cázares-Delgadillo J, Balaguer-Fernández C, Calatayud-Pascual A, Ganem-Rondero A, Quintanar-Guerrero D, López-Castellano AC, Merino V, Kalia YN. Transdermal iontophoresis of dexamethasone sodium phosphate in vitro and in vivo: Effect of experimental parameters and skin type on drug stability and transport kinetics. Eur J Pharm Biopharm 2010; 75:173-8. [PMID: 20332024].

60. Bose R, Spulber S, Kilian P, Heldring N, Lönnerberg P, Johnsson A, Conti M, Hermanson O, Ceccatelli S. Tet3 mediates stable glucocorticoid-induced alterations in DNA methylation and Dnmt3a/Dkk1 expression in neural progenitors. Cell Death Dis 2015; 6:e1793-.

61. Provençal N, Arloth J, Cattaneo A, Anacker C, Cattane N, Wiechmann T, Röh S, Ködel M, Klengel T, Czamara D, Müller NS, Lahti J, Räikkönen K, Pariante CM, Binder EB. Glucocorticoid exposure during hippocampal neurogenesis primes future stress response by inducing changes in DNA methylation. Proc Natl Acad Sci USA 2020; 117:23280- [PMID: 31399550].

62. Boettiger AN, Bintu B, Moffitt JR, Wang S, Beliveau BJ, Fudenberg G, Imakaev M, Mirny LA, Wu C-t, Zhuang X. Super-resolution imaging reveals distinct chromatin folding for different epigenetic states. Nature 2016; 529:418-22. [PMID: 26760202].

63. Sharma D, Bhave S, Gregg E, Uht R. Dexamethasone Induces a Putative Repressor Complex and Chromatin Modifications in the CRH Promoter. Mol Endocrinol 2013; 27:1142-52. [PMID: 23671328].

64. Pacaud R, Sery Q, Oliver L, Vallette FM, Tost J, Cartron P-F. DNMT3L interacts with transcription factors to target DNMT3L/DNMT3B to specific DNA sequences: Role of the DNMT3L/DNMT3B/p65-NFκB complex in the (de-)methylation of TRAF1. Biochimie 2014; 104:36-49. [PMID: 24952347].

65. Norvil AB, Petell CJ, Alabdi L, Wu L, Rossie S, Gowher H. Dnmt3b Methylates DNA by a Noncooperative Mechanism, and Its Activity Is Unaffected by Manipulations at the Predicted Dimer Interface. Biochemistry 2018; 57:4312-24. [PMID: 27768276].

66. Goya L, Maiyar AC, Ge Y, Firestone GL. Glucocorticoids induce a G1/G0 cell cycle arrest of Con8 rat mammary tumor cells that is synchronously reversed by steroid withdrawal or addition of transforming growth factor-alpha. Mol Endocrinol 1993; 7:1121-32. [PMID: 8247014].

67. Nasonkin IO, Merbs SL, Lazo K, Oliver VF, Brooks M, Patel K, Enke RA, Nellissery J, Jamrich M, Le YZ, Bharti K, Fariss RN, Rachel RA, Zack DJ, Rodriguez-Boulan EJ, Swaroop A. Conditional knockdown of DNA methyltransferase 1 reveals a key role of retinal pigment epithelium integrity in photoreceptor outer segment morphogenesis. Development 2013; 140:1330-41. [PMID: 23406904].

68. Nasonkin IO, Lazo K, Hambright D, Brooks M, Fariss R, Swaroop A. Distinct nuclear localization patterns of DNA methyltransferases in developing and mature mammalian retina. J Comp Neurol 2011; 519:1914-30. [PMID: 21452232].

69. Yu M, Bojic S, Figueiredo GS, Rooney P, de Havilland J, Dickinson A, Figueiredo FC, Lako M. An important role for adenine, cholera toxin, hydrocortisone and triiodothyronine in the proliferation, self-renewal and differentiation of limbal stem cells in vitro. Exp Eye Res 2016; 152:113-22. [PMID: 27693410].

70. Singh RK, Diaz PE, Binette F, Nasonkin IO. Immunohistochemical Detection of 5-Methylcytosine and 5-Hydroxymethylcytosine in Developing and Postmitotic Mouse Retina. J Vis Exp 2018; •••:e58274-.

71. Fürst R, Zahler S, Vollmar AM. Dexamethasone-Induced Expression of Endothelial Mitogen-Activated Protein Kinase Phosphatase-1 Involves Activation of the Transcription Factors Activator Protein-1 and 3′,5′-Cyclic Adenosine 5′-Monophosphate Response Element-Binding Protein and the Generation of Reactive Oxygen Species. Endocrinology 2008; 149:3635-42. [PMID: 18403484].

72. Liu W, Zhao Z, Na Y, Meng C, Wang J, Bai R. Dexamethasone-induced production of reactive oxygen species promotes apoptosis via endoplasmic reticulum stress and autophagy in MC3T3–E1 cells. Int J Mol Med 2018; 41:2028-36. [PMID: 29393368].

73. Iuchi T, Akaike M, Mitsui T, Ohshima Y, Shintani Y, Azuma H, Matsumoto T. Glucocorticoid excess induces superoxide production in vascular endothelial cells and elicits vascular endothelial dysfunction. Circ Res 2003; 92:81-7. [PMID: 12522124].

74. Deng S, Dai G, Chen S, Nie Z, Zhou J, Fang H, Peng H. Dexamethasone induces osteoblast apoptosis through ROS-PI3K/AKT/GSK3β signaling pathway. Biomed Pharmacother 2019; 110:602-8. [PMID: 30537677].

75. Qihan W, Xiaohua N. ROS-Mediated DNA Methylation Pattern Alterations in Carcinogenesis. Curr Drug Targets 2015; 16:13-9. [PMID: 25585126].

76. Quan X, Lim S-O, Jung G. Reactive oxygen species downregulate catalase expression via methylation of a CpG Island in the Oct-1 promoter. FEBS Lett 2011; 585:3436-41. [PMID: 21985966].

77. Lim S-O, Gu J-M, Kim MS, Kim H-S, Park YN, Park CK, Cho JW, Park YM, Jung G. Epigenetic Changes Induced by Reactive Oxygen Species in Hepatocellular Carcinoma: Methylation of the E-cadherin Promoter. Gastroenterology 2008; 135:2128-40. [PMID: 18801366].

78. McMonnies C. Reactive oxygen species, oxidative stress, glaucoma and hyperbaric oxygen therapy. J Optom 2018; 11:3-9. [PMID: 28760643].

79. Tezel G. Oxidative stress in glaucomatous neurodegeneration: mechanisms and consequences. Prog Retin Eye Res 2006; 25:490-513. [PMID: 16962364].

80. Izzotti A, Bagnis A, Saccà SC. The role of oxidative stress in glaucoma. Mutat Res Rev Mutat Res 2006; 612:105-14. [PMID: 16413223].

81. Samuel W, Jaworski C, Postnikova OA, Kutty RK, Duncan T, Tan LX, Poliakov E, Lakkaraju A, Redmond TM. Appropriately differentiated ARPE-19 cells regain phenotype and gene expression profiles similar to those of native RPE cells. Mol Vis 2017; 23:60-89. [PMID: 28356702].

82. Ahmado A, Carr A-J, Vugler AA, Ma S, Gias C, Lawrence JM, Chen LL, Chen FK, Turowski P, da Cruz L, Coffey PJ. Induction of Differentiation by Pyruvate and DMEM in the Human Retinal Pigment Epithelium Cell Line ARPE-19. Invest Ophthalmol Vis Sci 2011; 52:7148-59. [PMID: 21743014].

83. Dvoriantchikova G, Seemungal RJ, Ivanov D. The epigenetic basis for the impaired ability of adult murine retinal pigment epithelium cells to regenerate retinal tissue. Sci Rep 2019; 9:3860-[PMID: 30846751].

84. Stern J, Temple S. Retinal pigment epithelial cell proliferation. Exp Biol Med (Maywood) 2015; 240:1079-86. [PMID: 26041390].

85. Leff SR, Yarian DL, Shields JA, Masciulli L, Green SN. Tumor-associated retinal pigment epithelial proliferation simulating retinal pigment epithelial tear. Retina 1989; 9:267-9. [PMID: 2629042].

86. Perera A, Eisen D, Wagner M, Laube SK, Kunzel AF, Koch S, Steinbacher J, Schulze E, Splith V, Mittermeier N, Muller M, Biel M, Carell T, Michalakis S. TET3 is recruited by REST for context-specific hydroxymethylation and induction of gene expression. Cell Reports 2015; 11:283-94. [PMID: 25843715].

87. Phulke S, Kaushik S, Kaur S, Pandav SS. Steroid-induced Glaucoma: An Avoidable Irreversible Blindness. J Curr Glaucoma Pract 2017; 11:67-72. .

88. Srinivasan R, Sharma U, George R, Raman R, Sharma T. Intraocular Pressure Changes after Dexamethasone Implant in Patients with Glaucoma and Steroid Responders. Retina 2017; 39:157-162[PMID: 29095355].

89. Alkozi HA, Franco R, Pintor JJ. Epigenetics in the Eye: An Overview of the Most Relevant Ocular Diseases. Front Genet 2017; 8:144-[PMID: 29075285].

90. Pennington KL, DeAngelis MM. Epigenetic Mechanisms of the Aging Human Retina. J Exp Neurosci 2016; 9:Suppl 251-79. [PMID: 26966390].

91. Matsuda A, Asada Y, Takakuwa K, Sugita J, Murakami A, Ebihara N. DNA Methylation Analysis of Human Trabecular Meshwork Cells During Dexamethasone Stimulation. Invest Ophthalmol Vis Sci 2015; 56:3801-9. [PMID: 26066748].

92. Hornbeak DM, Thorne JE. Immunosuppressive therapy for eye diseases: Effectiveness, safety, side effects and their prevention. Taiwan J Ophthalmol 2015; 5:156-63. [PMID: 29018691].

93. Cooper AE, Cho J-H, Menges S, Masood S, Xie J, Yang J, Klassen H. Immunosuppressive Treatment Can Alter Visual Performance in the Royal College of Surgeons Rat. J Ocul Pharmacol Ther 2016; 32:296-303. [PMID: 27008099].

94. Zhou JY, Zhong HJ, Yang C, Yan J, Wang HY, Jiang JX. Corticosterone exerts immunostimulatory effects on macrophages via endoplasmic reticulum stress. Br J Surg 2010; 97:281-93. [PMID: 20069608].

95. Ugor E, Prenek L, Pap R, Berta G, Ernszt D, Najbauer J, Németh P, Boldizsár F, Berki T. Glucocorticoid hormone treatment enhances the cytokine production of regulatory T cells by upregulation of Foxp3 expression. Immunobiology 2018; 223:422-31. [PMID: 29223294].

96. Wang L, Liu Y, Beier UH, Han R, Bhatti TR, Akimova T, Hancock WW. Foxp3+ T-regulatory cells require DNA methyltransferase 1 expression to prevent development of lethal autoimmunity. Blood 2013; 121:3631-9. [PMID: 23444399].

97. Licht JD, Bennett RL. Leveraging epigenetics to enhance the efficacy of immunotherapy. Clin Epigenetics 2021; 13:115-[PMID: 34001289].